

# Upper-tropospheric relative humidity observations and implications for cirrus ice nucleation

Andrew J. Heymsfield, Larry M. Miloshevich, and Cynthia Twohy  
National Center for Atmospheric Research, Boulder, CO

Glen Sachse  
NASA Langley Research Center, Hampton, VA

Samuel Oltmans  
NOAA Climate Monitoring and Diagnostics Laboratory, Boulder, CO

**Abstract.** Relative humidity (RH) measurements acquired in orographic wave cloud and cirrus environments are used to investigate the temperature-dependent RH required to nucleate ice crystals in the upper troposphere,  $RH_{nuc}(T)$ . High ice-supersaturations in clear air — conducive to the maintenance of aircraft contrails yet below  $RH_{nuc}$  and therefore insufficient for cirrus formation — are not uncommon. Earlier findings are supported that  $RH_{nuc}$  in mid-latitude, continental environments decreases from water-saturation at temperatures above  $-39^{\circ}\text{C}$  to 75% RH at  $-55^{\circ}\text{C}$ . Uncertainty in determining  $RH_{nuc}$  below  $-55^{\circ}\text{C}$  results in part from size detection limitations of the microphysical instrumentation, but analysis of data from the SUCCESS experiment indicates that  $RH_{nuc}$  below  $-55^{\circ}\text{C}$  is between 70 and 88%. A small amount of data acquired off-shore suggests the possibility that  $RH_{nuc}$  may also depend on properties of the aerosols.

## 1. Introduction

Uncertainties in the radiation and moisture budgets in climate models result in part from inadequate knowledge of cirrus microphysical properties and the thermodynamic conditions required to nucleate cirrus ice crystals. This study examines the temperature-dependent relative humidity required to nucleate ice crystals in the upper troposphere,  $RH_{nuc}(T)$ . This condition determines cirrus initiation and frequency of occurrence, influences cirrus microphysical and radiative properties, and thereby influences cirrus effects on climate.

Ice-supersaturation in the upper troposphere has long been inferred from the observation of long-lasting aircraft contrails in otherwise clear air [e.g., Brewer, 1946], but only recently has instrumentation been capable of accurately measuring ice-supersaturation from aircraft at cold temperatures. The contrail shown in Fig. 1 was produced in ascending air upwind of an orographic wave cloud by the NASA DC-8 aircraft during SUCCESS (the “Subsonic aircraft: Contrail and Cloud Effects Special Study” experiment). Some de-

gree of ice-supersaturation must have been present in the clear air to maintain the contrail, but a higher ice-supersaturation must be required to produce ice crystals from the ambient aerosol population.

Heymsfield and Miloshevich [1995, hereafter “HM”] used measurements in orographic wave cloud and cirrus environments from FIRE-II (the First ISCCP Research Experiment, Phase II) to place upper and lower limits on  $RH_{nuc}$  in the temperature range  $-35$  to  $-55^{\circ}\text{C}$ . Orographic wave clouds are well-suited for studying ice nucleation because the airflow is relatively laminar and the RH increases continuously via vertical lifting toward  $RH_{nuc}$  at the upwind cloud boundary. Furthermore, ice crystals in wave clouds are carried downwind rather than falling through the ascending air as in cirrus, allowing the ice nucleation conditions to be sampled repeatedly [Heymsfield and Miloshevich, 1993]. The peak RH observed during penetrations into the upwind edge of wave clouds occurs when the vapor depletion rate from growth of recently-nucleated ice crystals is equal to the vapor supply rate from cooling due to vertical velocities of several  $\text{m s}^{-1}$ , and represents an upper limit to  $RH_{nuc}$  since ice crystals must have nucleated prior to the peak and therefore at a lower RH. HM found that these peak RH values — their empirical “ $RH_{hn}(T)$ ” curve — varied from water-saturation at temperatures above  $-39^{\circ}\text{C}$  to 75% RH (with respect to water) at  $-55^{\circ}\text{C}$ . HM also determined a lower bound on  $RH_{nuc}$  in the temperature range  $-35$  to  $-47^{\circ}\text{C}$  — about 10% below the  $RH_{hn}$  curve — based on the maximum RH measured in “clear air” in a non-orographic environment during FIRE-II. In this article we use RH and microphysical data from balloon launches near Boulder, Colorado and from the FIRE-II and SUCCESS experiments to further explore bounds on  $RH_{nuc}(T)$ , particularly at colder temperatures. Most data presented in this paper represent mid-latitude, continental, non-convective environments.

## 2. Observed Ice Nucleation Conditions

### 2.1. Balloon-borne Measurements

Ice-supersaturations of 20-30% have been observed in clear air and in regions of low ice crystal concentration near the tops of cirrus [HM]. RH measurements are shown in Fig. 2 from monthly launches of the NOAA balloon-borne cryogenic hygrometer [Oltmans



Figure 1. Contrail produced upwind of an orographic wave cloud near Boulder, Colorado on 2 May 1996. Photo courtesy of Dan Breed (NCAR/MMM).

and Hoffman, 1995]. The highest RH points below  $-40^{\circ}\text{C}$  are consistent with  $RH_{hn}$ , within the instrument's estimated accuracy of 5-10%. Although these launches were preferentially conducted in clear-air conditions, some launches are known to have passed through cirrus and therefore the data does not necessarily represent  $RH_{nuc}$ . However, Fig. 2 demonstrates that high ice-supersaturations are not uncommon.

## 2.2. FIRE-II

Clear-air RH data from FIRE-II (not previously reported by HM) are shown in Fig. 3A, where in this case "clear air" means an absence of ice crystals larger than the  $50\ \mu\text{m}$  detection threshold of a Particle Measuring Systems 2D-C probe for at least two seconds prior to and after an accepted data point. Since the detection threshold of the 2D-C probe is so large, data points that lie above the  $RH_{hn}$  curve were examined using simultaneous particle collection data from a Video Ice Particle Sampler (VIPS) [McFarquhar and Heymsfield, 1996]. These points were either verified to be free of ice crystals larger than the  $5\text{-}10\ \mu\text{m}$  detection threshold of

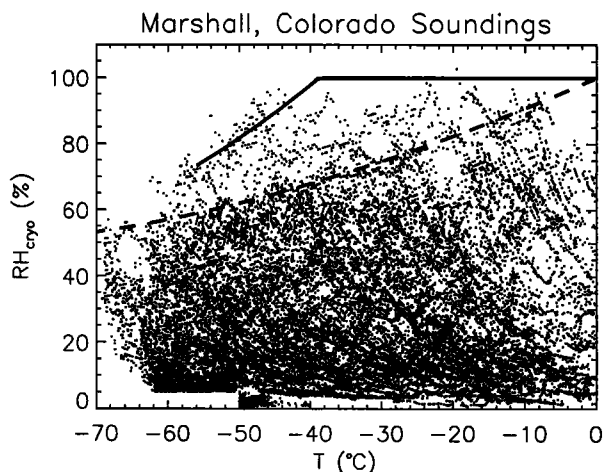


Figure 2. RH measurements from the NOAA cryogenic hygrometer for monthly balloon launches between 1991 and 1996 near Boulder, Colorado, shown as a function of temperature. Solid line is  $RH_{hn}$  from HM; dashed line is ice-saturation.

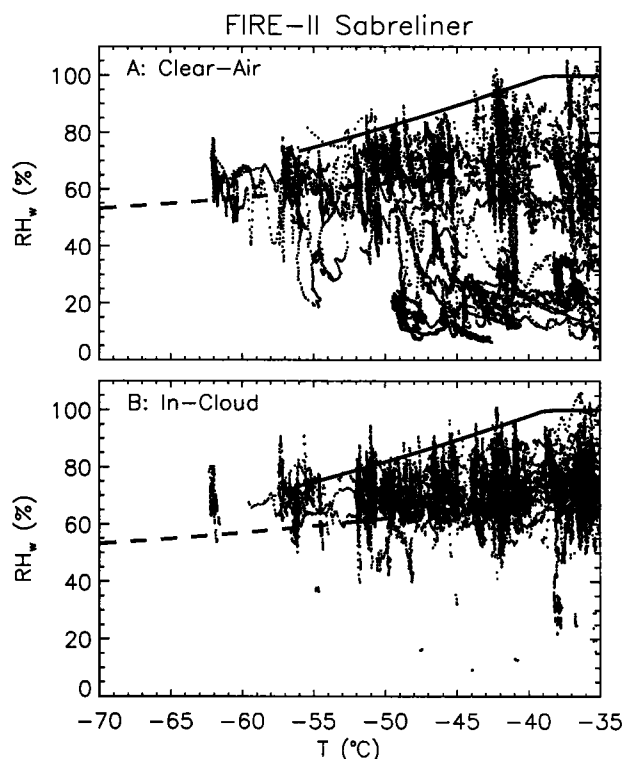


Figure 3. RH measurements from a cryogenic hygrometer on the NCAR Sabreliner aircraft during FIRE-II, shown as a function of temperature. Panel A: clear-air data as determined from 2D-C measurements; Panel B: in-cloud data. Solid line is  $RH_{hn}$ ; dashed line is ice-saturation.

the VIPS, or the images showed extremely low ice crystal concentrations. The accuracy of the NCAR cryogenic hygrometer used to make the RH measurements is  $\pm 1^{\circ}\text{C}$  in the frost-point temperature, or about 10% in RH at upper-tropospheric air temperatures [HM].

The highest clear-air RH data points are 5-7% above  $RH_{hn}$  over the temperature range for which  $RH_{hn}$  is defined. The RH at  $-62^{\circ}\text{C}$  in Fig. 3A reaches 78%, therefore  $RH_{nuc}$  is not given by extrapolation of the  $RH_{hn}$  curve below  $-55^{\circ}\text{C}$ . However, slow ice crystal growth rates at cold temperatures may have resulted in an erroneous "clear air" classification of some high-RH points since undetectable ice crystals smaller than  $5\text{-}10\ \mu\text{m}$  may have recently nucleated. If so, the resulting overestimate of  $RH_{nuc}$  should be small relative to wave cloud environments because the vertical velocities are lower and therefore the increase in RH while crystals grow to detectable sizes is less. The in-cloud cirrus data (Fig. 3B) demonstrate that the RH can increase substantially above  $RH_{nuc}$ . High in-cloud RH values are more likely to occur when the vertical velocity (and hence the vapor supply rate) is high, or when the ice crystals are small or the temperature is low, both of which result in slow ice crystal growth rates and therefore low vapor depletion rates.

## 2.3. SUCCESS

Figure 4 shows RH in clear air measured by a diode laser hygrometer (DLH) [Vay et al., 1997] for three flights during SUCCESS, where in this case "clear air"

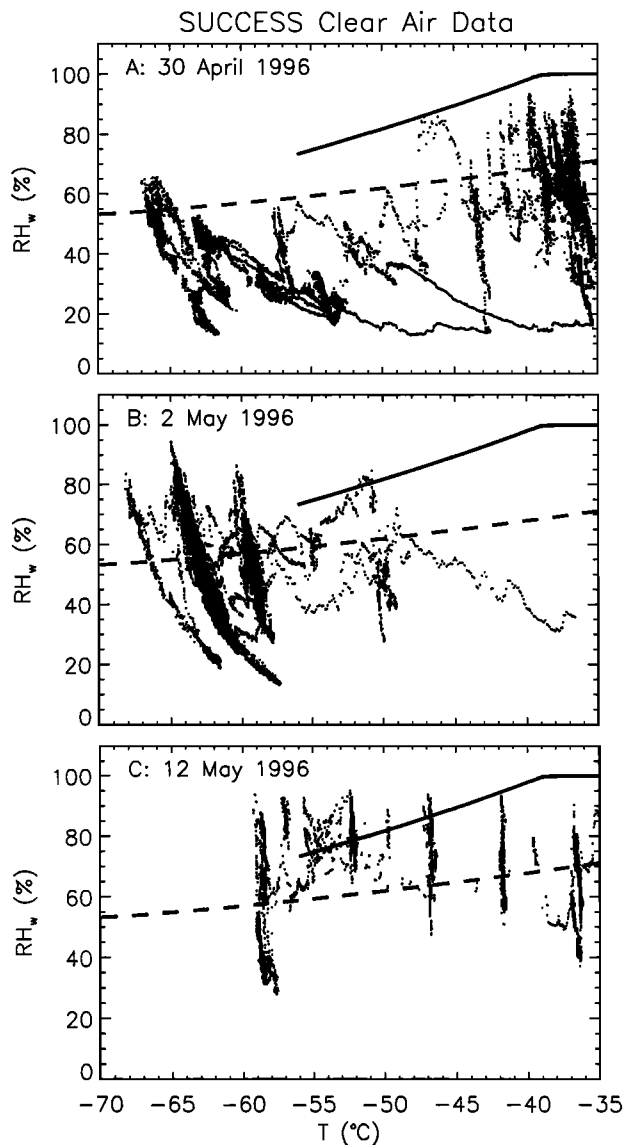


**Figure 4.** RH derived from DLH water vapor measurements in “clear air” (as determined by the CVI) from three research flights during SUCCESS, shown as a function of temperature. Solid line is  $RH_{hn}$ ; dashed line is  $RH_i$ .

means an absence of ice crystals detected by a Counterflow Virtual Impactor (CVI) [Twohy *et al.*, 1996] for at least 2 seconds prior to and after an accepted data point. The detection threshold of the CVI varied between 5 and 15  $\mu\text{m}$  diameter depending on the instrument settings, but was usually 5  $\mu\text{m}$ . The accuracy of the RH derived from DLH water vapor measurements and air temperature measurements is estimated to be 6–8%, based on the difference between the derived RH and ice-saturation ( $RH_i$ ) during penetrations into wave clouds and contrails (where HM calculated that the equilibrium RH in vertical velocities up to several  $\text{m s}^{-1}$  is within 1–2% of  $RH_i$  if the concentration of small ice crystals is several  $\text{cm}^{-3}$  or greater).

Clear air upwind of orographic wave clouds was sampled on 30 April over eastern New Mexico at temperatures between  $-35$  and  $-41^\circ\text{C}$  (Fig. 4A). The peak RH values of about 95% were comparable to  $RH_{hn}$ , but the

highest RH regions may not have been penetrated since the aircraft was restricted to fly primarily normal rather than parallel to the wind direction, although the data were acquired immediately upwind of the visible cloud edge where the highest RH values would be expected.

The orographic wave environment sampled on the lee side of the Rocky Mountains on 2 May at temperatures between  $-57$  and  $-65^\circ\text{C}$  (Fig. 4B) showed clear-air RH values approaching water-saturation, seemingly inconsistent with the FIRE-II and balloon-borne measurements. As explored in Section 3, ice nucleation (and  $RH_{nuc}$ ) likely preceded the peak RH because the vertical velocities are high ( $\sim 2.5 \text{ m s}^{-1}$ ) and ice crystal growth rates at  $-65^\circ\text{C}$  are very slow (about a factor of 7 slower than at  $-55^\circ\text{C}$ ), implying a relatively rapid increase in RH above  $RH_{nuc}$  during the time when newly-nucleated ice crystals grew to detectable sizes.

The off-shore, non-wave environment sampled off the California coast on 12 May (Fig. 4C) provides clear-air data at low temperatures when the vertical velocities were lower than in Fig. 4B (generally  $< 1 \text{ m s}^{-1}$ ), and therefore the degree to which the peak RH exceeds  $RH_{nuc}$  should be less severe. The peak RH exceeded 90% and was essentially independent of temperature, much different than the previously-observed consistency with  $RH_{hn}$  above  $-55^\circ\text{C}$ . Measured ice nucleus (IN) and condensation nucleus (CN) concentrations were low on this flight relative to continental measurements on other research days, and the chemical composition of the IN was higher in sulfates than the mineral materials that dominated the continental measurements [P. DeMott, personal communication]. The different characteristics of the IN and CN in this airmass suggest that  $RH_{nuc}$  may depend on aerosol properties.

### 3. Discussion and Implications

The RH data presented in Section 2, with the exception of Fig. 4C, show that  $RH_{nuc}(T)$  is generally consistent with HM’s  $RH_{hn}(T)$  curve at temperatures above  $-55^\circ\text{C}$ . The high RH values at  $-60^\circ\text{C}$  and below in Figs. 3A and 4B indicate that  $RH_{nuc}$  below  $-55^\circ\text{C}$  is not an extrapolation of  $RH_{hn}$  to colder temperatures. This section will emphasize interpretation of the high RH measurements at cold temperatures, particularly those in Figs. 4B and 4C.

The basis for suggesting that the peak RH in a wave environment at cold temperatures may substantially exceed  $RH_{nuc}$  is illustrated in Fig. 5, which shows time series of RH and ice crystal concentration above 5–15  $\mu\text{m}$  diameters for the wave cloud penetration that corresponds to the highest RH values seen in Fig. 4B. The peak RH (labeled “S<sup>\*</sup>”) — the point at which vapor depletion from growing ice crystals balances vapor supply from vertical lifting — occurs well before the crystals are detectable by the VIPS, CVI, and a PVM-100. Detection of crystals larger than 2  $\mu\text{m}$  diameter by a Multiangular Aerosol Spectrometer Probe (MASP) confirms that ice nucleation occurred prior to the peak RH, and therefore  $RH_{nuc}$  at  $-65^\circ\text{C}$  must be below 88%.

The average calculated ice crystal growth rate at  $-65^\circ\text{C}$  for ice crystal diameters between 0.1 and 5  $\mu\text{m}$  is  $0.045 \mu\text{m s}^{-1}$  if the RH is 94% (the peak value in Fig. 5), and is  $0.03 \mu\text{m s}^{-1}$  at 80% RH and  $0.02 \mu\text{m s}^{-1}$  at 70% RH (the RH upwind of the wave). Ice crystals ex-

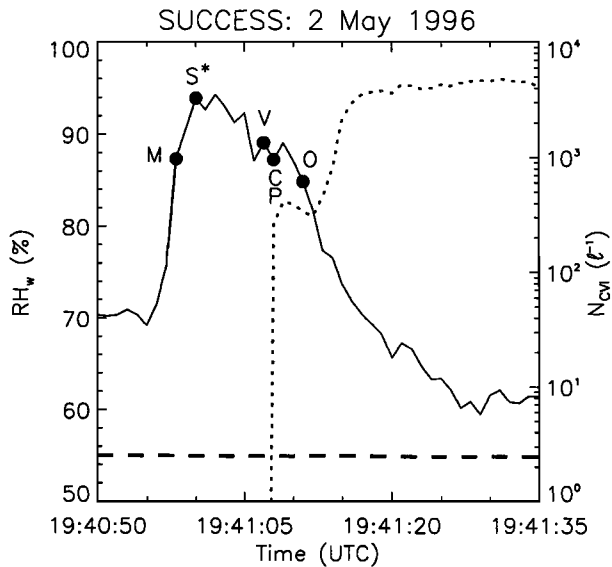


**Figure 5.** Time series of RH measured by the DLH (solid curve) and ice crystal concentration measured by the CVI (short dashes) for a wave cloud penetration at  $-65^{\circ}\text{C}$ . Relative to the peak RH (“S\*”), the first detection of ice crystals is indicated from the VIPS (“V”), the CVI (“C”), the PVM-100 (“P”), and the MASP (“M”). Bold dashed line is  $RH_i$ .

isted but were smaller than  $5\ \mu\text{m}$  for on the order of 150 s (assuming a constant ice crystal growth rate at about 80% RH). Neglecting vapor depletion, for a vertical velocity of  $1.5\ \text{m s}^{-1}$  the RH would increase above  $RH_{nuc}$  by about 20% in 150 s. Unfortunately, it is impossible to estimate  $RH_{nuc}$  from such calculations because the aircraft was not flying along the wind direction during this penetration. At the minimum, it is apparent from Fig. 5 that  $RH_{nuc}$  at  $-65^{\circ}\text{C}$  lies somewhere between 70% and 88%, and is likely below 88% considering the time required for crystals to grow to  $2\ \mu\text{m}$ .

The very high RH values observed during the 12 May SUCCESS case (Fig. 4C) are somewhat unexpected because the vertical velocities (and vapor supply rates) were relatively low. This case is also inconsistent with  $RH_{hn}$  above  $-55^{\circ}\text{C}$ , where ice crystal growth rates are faster and instrument detection threshold limitations should be less problematic. We speculate that  $RH_{nuc}$  may be greater in this “maritime” environment than in a continental environment as a result of different aerosol properties, based in part on the lower IN and CN concentrations and different IN chemical composition measured on this flight relative to the 2 May flight. Numerous factors could lead to differing aerosol properties in a maritime air mass, such as fewer sources of aerosols (e.g., surface sources of mineral materials and jet aircraft exhaust), or removal of aerosols via fallout of previously-formed ice crystals, such that ice nucleation from the remaining less-numerous or less-effective aerosols requires higher ice-supersaturations.

#### 4. Summary and Conclusions

The RH measurements presented in this paper and in HM indicate that high ice-supersaturations in the upper troposphere are not uncommon, both in clear air and

in clouds. The FIRE-II and balloon-borne data show that the cirrus ice nucleation condition,  $RH_{nuc}(T)$ , is consistent with HM’s  $RH_{hn}(T)$  curve in continental environments down to  $-55^{\circ}\text{C}$ , but  $RH_{hn}$  should not be extrapolated to lower temperatures. The SUCCESS data indicate that  $RH_{nuc}$  below  $-55^{\circ}\text{C}$  is between 70 and 88%.  $RH_{nuc}$  may also depend on characteristics of the aerosols. Perhaps a minimum of two  $RH_{nuc}$  relations are needed — representing continental and maritime air masses — but much more data are needed to assess particularly the maritime relation. Uncertainty in observing  $RH_{nuc}$  increases at cold temperatures because ice crystal growth rates are very slow and the RH may rise substantially before ice crystals are detectable by most microphysical instrumentation. A well-conceived experiment in orographic wave clouds, with accurate RH measurements and microphysical instrumentation with a submicron detection threshold, may provide a relatively simple dynamical environment for further study of continental ice nucleation conditions.

**Acknowledgments.** This study was supported by the following programs: NASA FIRE-III grant L55549D; NASA SUCCESS grant A49760D; Air Force Office of Scientific Research grant F49620-96-C-0024.

#### References

- Brewer, A.W., Condensation trails. *Weather*, 1, 34-40.
- Heymsfield, A.J., and L.M. Miloshevich, Homogeneous ice nucleation and supercooled liquid water in orographic wave clouds. *J. Atmos. Sci.*, 50, 2335-2353, 1993.
- Heymsfield, A.J., and L.M. Miloshevich, Relative humidity and temperature influences on cirrus formation and evolution: Observations from wave clouds and FIRE-II. *J. Atmos. Sci.*, 52, 4302-4326, 1995.
- McFarquhar, G.M., and A.J. Heymsfield, Microphysical characteristics of three anvils sampled during the Central Equatorial Pacific Experiment. *J. Atmos. Sci.*, 53, 2401-2423, 1996.
- Oltmans, S.J., and D.J. Hofmann, Increase in lower stratospheric water vapour at a mid-latitude Northern Hemisphere site from 1981 to 1994. *Nature*, 374, 146-149, 1995.
- Twohy, C.H., A.J. Schanot, and W.A. Cooper, Measurement of condensed water content in liquid and ice clouds using an airborne counterflow virtual impactor. *J. Atmos. Ocean. Tech.*, 14, 197-202, 1996.
- Vay, S.A., B.E. Anderson, G.W. Sachse, J.E. Collins, J.R. Podolske, C.H. Twohy, B.W. Gandrud, B.L. Gary, K.R. Chan, S.L. Baughcum, and H.A. Wallio, DC-8-based observations of aircraft CO, CH<sub>4</sub>, N<sub>2</sub>O, and H<sub>2</sub>O(g) emission indices during SUCCESS. Submitted to *Geophys. Res. Lett.*, 1997.
- A.J. Heymsfield, L.M. Miloshevich, and C. Twohy, National Center for Atmospheric Research P.O. Box 3000 Boulder, Colorado 80307. (e-mail: heyms1@ncar.ucar.edu)
- G. Sachse, NASA Langley Research Center 5 North Dryden Street Hampton, Virginia 23681.
- S. Oltmans, NOAA Climate Monitoring and Diagnostics Laboratory 325 Broadway Boulder, Colorado 80303.

(Received July 18, 1997; revised November 25, 1997; accepted December 5, 1997.)